

## 30. RADIOACTIVITY AND RADIATION PROTECTION

Revised August 2011 by S. Roesler and M. Silari (CERN).

## 30.1. Definitions [1,2]

## 30.1.1. Physical quantities :

• **Fluence**,  $\Phi$  (unit:  $1/\text{m}^2$ ): The fluence is the quotient of  $dN$  by  $da$ , where  $dN$  is the number of particles incident upon a small sphere of cross-sectional area  $da$

$$\Phi = dN/da . \quad (30.1)$$

In dosimetric calculations, fluence is frequently expressed in terms of the lengths of the particle trajectories. It can be shown that the fluence,  $\Phi$ , is given by

$$\Phi = dl/dV,$$

where  $dl$  is the sum of the particle trajectory lengths in the volume  $dV$ .

• **Absorbed dose**,  $D$  (unit: gray,  $1 \text{ Gy}=1 \text{ J/kg}=100 \text{ rad}$ ): The absorbed dose is the energy imparted by ionizing radiation in a volume element of a specified material divided by the mass of this volume element.

• **Kerma**,  $K$  (unit: gray): Kerma is the sum of the initial kinetic energies of all charged particles liberated by indirectly ionizing radiation in a volume element of the specified material divided by the mass of this volume element.

• **Linear energy transfer**,  $L$  or  $LET$  (unit:  $\text{J/m}$ , often given in  $\text{keV}/\mu\text{m}$ ): The linear energy transfer is the mean energy,  $dE$ , lost by a charged particle owing to collisions with electrons in traversing a distance  $dl$  in matter. *Low-LET radiation*: x rays and gamma rays (accompanied by charged particles due to interactions with the surrounding medium) or light charged particles such as electrons that produce sparse ionizing events far apart at a molecular scale ( $L < 10 \text{ keV}/\mu\text{m}$ ). *High-LET radiation*: neutrons and heavy charged particles that produce ionizing events densely spaced at a molecular scale ( $L > 10 \text{ keV}/\mu\text{m}$ ).

• **Activity**,  $A$  (unit: becquerel,  $1 \text{ Bq}=1/\text{s}=27 \text{ picocurie}$ ): Activity is the expectation value of the number of nuclear decays occurring in a given quantity of material per unit time.

## 30.1.2. Protection quantities :

Protection quantities are dose quantities developed for radiological protection that allow quantification of the extent of exposure of the human body to ionizing radiation from both whole and partial body external irradiation and from intakes of radionuclides.

• **Organ absorbed dose**,  $D_T$  (unit: gray): The mean absorbed dose in an organ or tissue  $T$  of mass  $m_T$  is defined as

$$D_T = \frac{1}{m_T} \int_{m_T} D dm .$$

• **Equivalent dose**,  $H_T$  (unit: sievert,  $1 \text{ Sv}=100 \text{ rem}$ ): The equivalent dose  $H_T$  in an organ or tissue  $T$  is equal to the sum of the absorbed doses  $D_{T,R}$  in the organ or

## 2 30. Radioactivity and radiation protection

tissue caused by different radiation types  $R$  weighted with so-called radiation weighting factors  $w_R$ :

$$H_T = \sum_R w_R \times D_{T,R} . \quad (30.2)$$

It expresses long-term risks (primarily cancer and leukemia) from low-level chronic exposure. The values for  $w_R$  recommended by ICRP [2] are given in Table 30.1.

**Table 30.1:** Radiation weighting factors,  $w_R$ .

| Radiation type                                 | $w_R$   |
|--|---|
| Photons, electrons and muons                   | 1   |
| Neutrons, $E_n < 1$ MeV                        | $2.5 + 18.2 \times \exp[-(\ln E_n)^2/6]$      |
| 1 MeV $\leq E_n \leq 50$ MeV                   | $5.0 + 17.0 \times \exp[-(\ln(2E_n))^2/6]$    |
| $E_n > 50$ MeV                                 | $2.5 + 3.25 \times \exp[-(\ln(0.04E_n))^2/6]$ |
| Protons and charged pions                      | 2   |
| Alpha particles, fission fragments, heavy ions | 20  |

• **Effective dose,  $E$**  (unit: sievert): The sum of the equivalent doses, weighted by the tissue weighting factors  $w_T$  ( $\sum_T w_T = 1$ ) of several organs and tissues  $T$  of the body that are considered to be most sensitive [2], is called “effective dose”:

$$E = \sum_T w_T \times H_T . \quad (30.3)$$

### 30.1.3. Operational quantities :

The body-related protection quantities, equivalent dose and effective dose, are not measurable in practice. Therefore, operational quantities are used for the assessment of effective dose or mean equivalent doses in tissues or organs. These quantities aim to provide a conservative estimate for the value of the protection quantity.

• **Ambient dose equivalent,  $H^*(10)$**  (unit: sievert): The dose equivalent at a point in a radiation field that would be produced by the corresponding expanded and aligned field in a 30 cm diameter sphere of unit density tissue (ICRU sphere) at a depth of 10 mm on the radius vector opposing the direction of the aligned field. Ambient dose equivalent is the operational quantity for *area monitoring*.

• **Personal dose equivalent,  $H_p(d)$**  (unit: sievert): The dose equivalent in ICRU tissue at an appropriate depth,  $d$ , below a specified point on the human body. The specified point is normally taken to be where the individual dosimeter is worn. For the assessment of effective dose,  $H_p(10)$  with a depth  $d = 10$  mm is chosen, and for the assessment of the dose to the skin and to the hands and feet the personal dose equivalent,  $H_p(0.07)$ , with a depth  $d = 0.07$  mm, is used. Personal dose equivalent is the operational quantity for *individual monitoring*.

#### 30.1.4. Dose conversion coefficients :

Dose conversion coefficients allow direct calculation of protection or operational quantities from particle fluence and are functions of particle type, energy and irradiation configuration. The most common coefficients are those for effective dose and ambient dose equivalent. The former are based on simulations in which the dose to organs of anthropomorphic phantoms is calculated for approximate actual conditions of exposure, such as irradiation of the front of the body (antero-posterior irradiation) or isotropic irradiation.

Conversion coefficients from fluence to effective dose are given for anterior-posterior irradiation and various particles in Fig. 30.1 [3]. For example, the effective dose from an anterior-posterior irradiation in a field of 1-MeV neutrons with a fluence of 1 neutron per  $\text{cm}^2$  is about 290 pSv. In Monte Carlo simulations such coefficients allow multiplication with fluence at scoring time such that effective dose to a human body at the considered location is directly obtained.

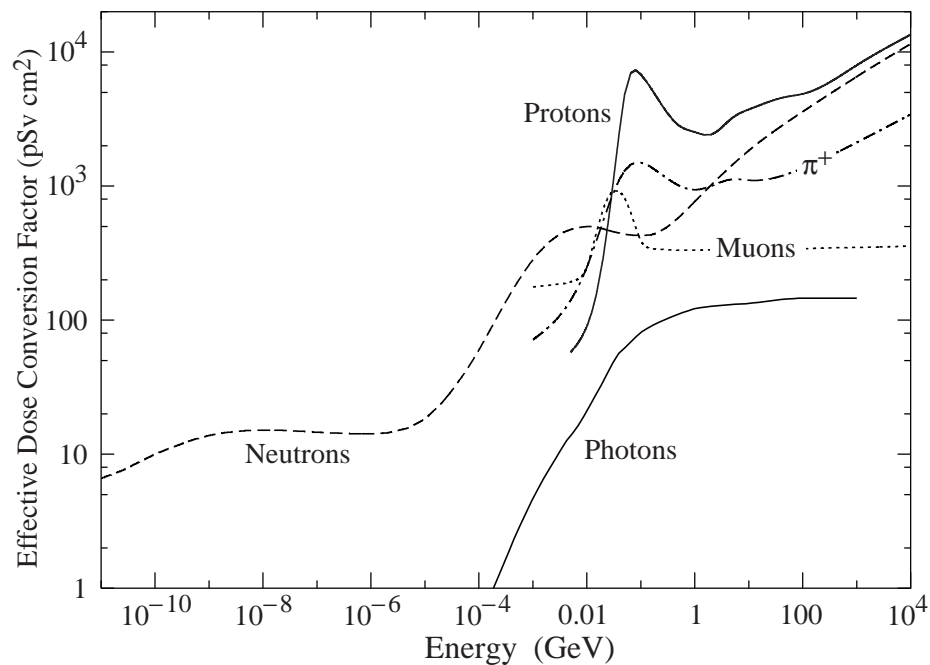


**Figure 30.1:** Fluence to effective dose conversion coefficients for anterior-posterior irradiation and various particles [3].

## 4 30. Radioactivity and radiation protection

### 30.2. Radiation levels [4]

- **Natural background radiation:** On a worldwide average, the annual whole-body dose equivalent due to all sources of natural background radiation ranges from 1.0 to 13 mSv (0.1–1.3 rem) with an annual average of 2.4 mSv [5]. In certain areas values up to 50 mSv (5 rem) have been measured. A large fraction (typically more than 50%) originate from inhaled natural radioactivity, mostly radon and radon daughters. The latter can vary by more than one order of magnitude: it is 0.1–0.2 mSv in open areas, 2 mSv on average in a house and more than 20 mSv in poorly ventilated mines.
- **Cosmic ray background radiation:** At sea level, the whole-body dose equivalent due to cosmic ray background radiation is dominated by muons; at higher altitudes also nucleons contribute. Dose equivalent rates range from less than 0.1  $\mu\text{Sv/h}$  at sea level to a few  $\mu\text{Sv/h}$  at aircraft altitudes. Details on cosmic ray fluence levels are given in the Cosmic Rays section (Sec. 24 of this *Review*).
- **Fluence to deposit one Gy:** *Charged particles:* The fluence necessary to deposit a dose of one Gy (in units of  $\text{cm}^{-2}$ ) is about  $6.24 \times 10^9 / (dE/dx)$ , where  $dE/dx$  (in units of  $\text{MeV g}^{-1} \text{cm}^2$ ) is the mean energy loss rate that may be obtained from Figs. 27.2 and 27.4 in Sec. 27 of this *Review*, and from <http://pdg.lbl.gov/AtomicNuclearProperties>. For example, it is approximately  $3.5 \times 10^9 \text{ cm}^{-2}$  for minimum-ionizing singly-charged particles in carbon. *Photons:* This fluence is about  $6.24 \times 10^9 / (Ef/\ell)$  for photons of energy  $E$  (in MeV), an attenuation length  $\ell$  (in  $\text{g cm}^{-2}$ ), and a fraction  $f \lesssim 1$ , expressing the fraction of the photon energy deposited in a small volume of thickness  $\ll \ell$  but large enough to contain the secondary electrons. For example, it is approximately  $2 \times 10^{11} \text{ cm}^{-2}$  for 1 MeV photons on carbon ( $f \approx 1/2$ ).

### 30.3. Health effects of ionizing radiation

Radiation can cause two types of health effects, deterministic and stochastic:

- **Deterministic effects** are tissue reactions which cause injury to a population of cells if a given threshold of absorbed dose is exceeded. The severity of the reaction increases with dose. The quantity in use for tissue reactions is the absorbed dose,  $D$ . When particles other than photons and electrons (low-*LET* radiation) are involved, a Relative Biological Effectiveness (*RBE*)-weighted dose may be used. The *RBE* of a given radiation is the reciprocal of the ratio of the absorbed dose of that radiation to the absorbed dose of a reference radiation (usually x rays) required to produce the same degree of biological effect. It is a complex quantity that depends on many factors such as cell type, dose rate, fractionation, etc.
- **Stochastic effects** are malignant diseases and heritable effects for which the probability of an effect occurring, but not its severity, is a function of dose without threshold.
- **Lethal dose:** The whole-body dose from penetrating ionizing radiation resulting in 50% mortality in 30 days (assuming no medical treatment) is 2.5–4.5 Gy (250–450 rad)<sup>†</sup>, as measured internally on the body longitudinal center line. The surface dose varies due to variable body attenuation and may be a strong function of energy.

---

<sup>†</sup> *RBE*-weighted when necessary

- **Cancer induction:** The cancer induction probability is about 5% per Sv on average for the entire population [2].
- **Recommended effective dose limits:** The International Commission on Radiological Protection (ICRP) recommends a limit for radiation workers of 20 mSv effective dose per year averaged over 5 years, with the provision that the dose should not exceed 50 mSv in any single year [2]. The limit in the EU-countries and Switzerland is 20 mSv per year, in the U.S. it is 50 mSv per year (5 rem per year). Many physics laboratories in the U.S. and elsewhere set lower limits. The effective dose limit for general public is typically 1 mSv per year.

### 30.4. Prompt neutrons at accelerators

Neutrons dominate the particle environment outside thick shielding (*e.g.*, > 1 m of concrete) for high energy (> a few hundred MeV) electron and hadron accelerators.

#### 30.4.1. *Electron accelerators* :

At electron accelerators, neutrons are generated via photonuclear reactions from bremsstrahlung photons. In the photon energy range from threshold (few MeV) to about 30 MeV, neutron production is via the Giant Dipole Resonance (GDR) mechanism. The reaction consists in a collective excitation of the nucleus, in which neutrons and protons oscillate in the direction of the photon electric field. The oscillation is damped by friction in a few cycles, with the photon energy being transferred to the nucleus in a process similar to evaporation. Nucleons emitted in the dipolar interaction have an anisotropic angular distribution, with a maximum at  $90^\circ$ , while those leaving the nucleus as a result of evaporation are emitted isotropically with a Maxwellian energy distribution described as [6]:

$$\frac{dN}{dE_n} = \frac{E_n}{T^2} e^{-E_n/T} , \quad (30.4)$$

where  $T$  is a nuclear ‘temperature’ (in units of MeV) characteristic of the particular target nucleus and its excitation energy. For heavy nuclei the ‘temperature’ generally lies in the range of  $T = 0.5\text{--}1.0$  MeV. For higher energy photons, the quasi-deuteron (between about 30 MeV and 250 MeV), delta resonance (250 MeV–1.2 GeV) and vector meson dominance ( $\gtrsim 1.2$  GeV) mechanisms become important.

Neutron yields from semi-infinite targets per kW of electron beam power are plotted in Fig. 30.2 as a function of the electron beam energy [6].

Typical neutron energy spectra outside of concrete (80 cm thick,  $2.35\text{ g/cm}^3$ ) and iron (40 cm thick) shields are shown in Fig. 30.3. In order to compare these spectra to those caused by proton beams (see below) the spectra are scaled by a factor of 100, which roughly corresponds to the difference in the high energy hadronic cross sections for photons and hadrons (*e.g.*, the fine structure constant). The shape of these spectra are generally characterized by a low-energy peak at around 1 MeV (evaporation neutrons) and a high-energy shoulder at around 70–80 MeV. In case of concrete shielding, the spectrum also shows a pronounced peak at thermal neutron energies.

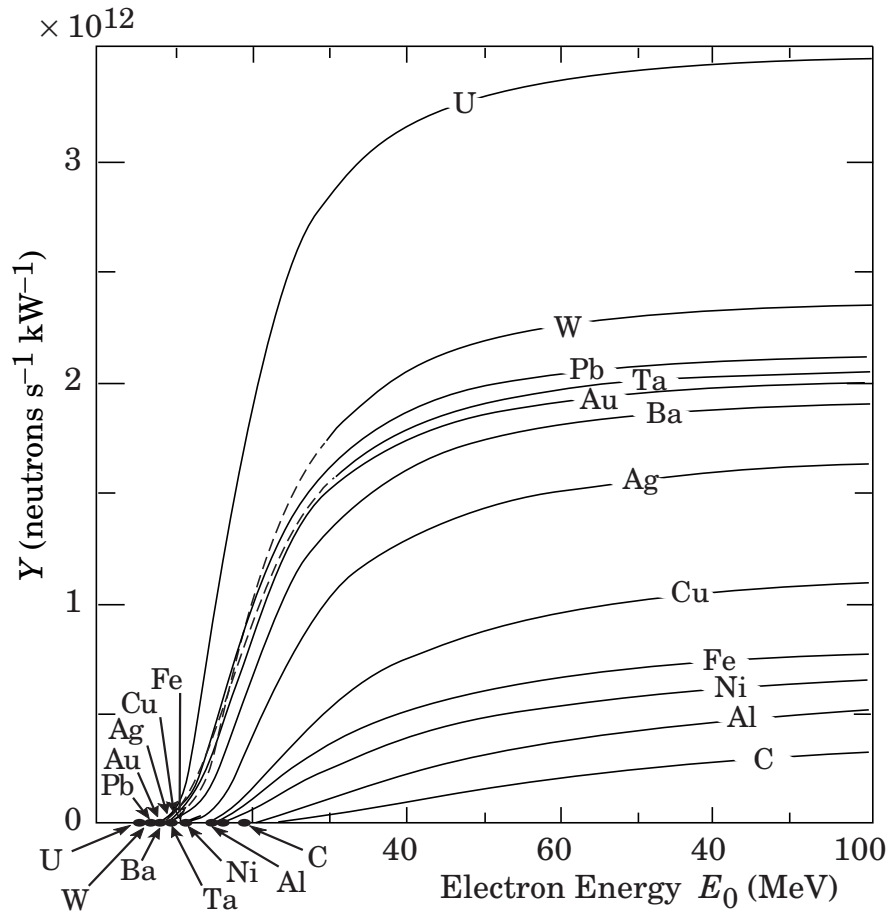


**Figure 30.2:** Neutron yields from semi-infinite targets per kW of electron beam power, as a function of the electron beam energy, disregarding target self-shielding [6].

#### 30.4.2. Proton accelerators :

At proton accelerators, neutron yields emitted per incident proton by different target materials are roughly independent of proton energy between 20 MeV and 1 GeV, and are given by the ratio C : Al : Cu-Fe : Sn : Ta-Pb = 0.3 : 0.6 : 1.0 : 1.5 : 1.7 [9]. Above about 1 GeV, the neutron yield is proportional to  $E^m$ , where  $0.80 \leq m \leq 0.85$  [10].

Typical neutron energy spectra outside of concrete and iron shielding are shown in Fig. 30.3. Here, the radiation fields are caused by a 25 GeV proton beam interacting with a thick copper target. The comparison of these spectra with those for an electron beam of the same energy reflects the difference in the hadronic cross sections between photons and hadrons above a few 100 MeV. Differences are increasing towards lower energies because of different interaction mechanisms. Furthermore, the slight shift in energy above about 100 MeV follows from the fact that the energies of the interacting photons are lower than 25 GeV. Apart from this the shapes of the two spectra are similar.

The neutron-attenuation length is shown in Fig. 30.4 for concrete and mono-energetic broad-beam conditions. As can be seen in the figure it reaches a value of about  $117 \text{ g/cm}^2$

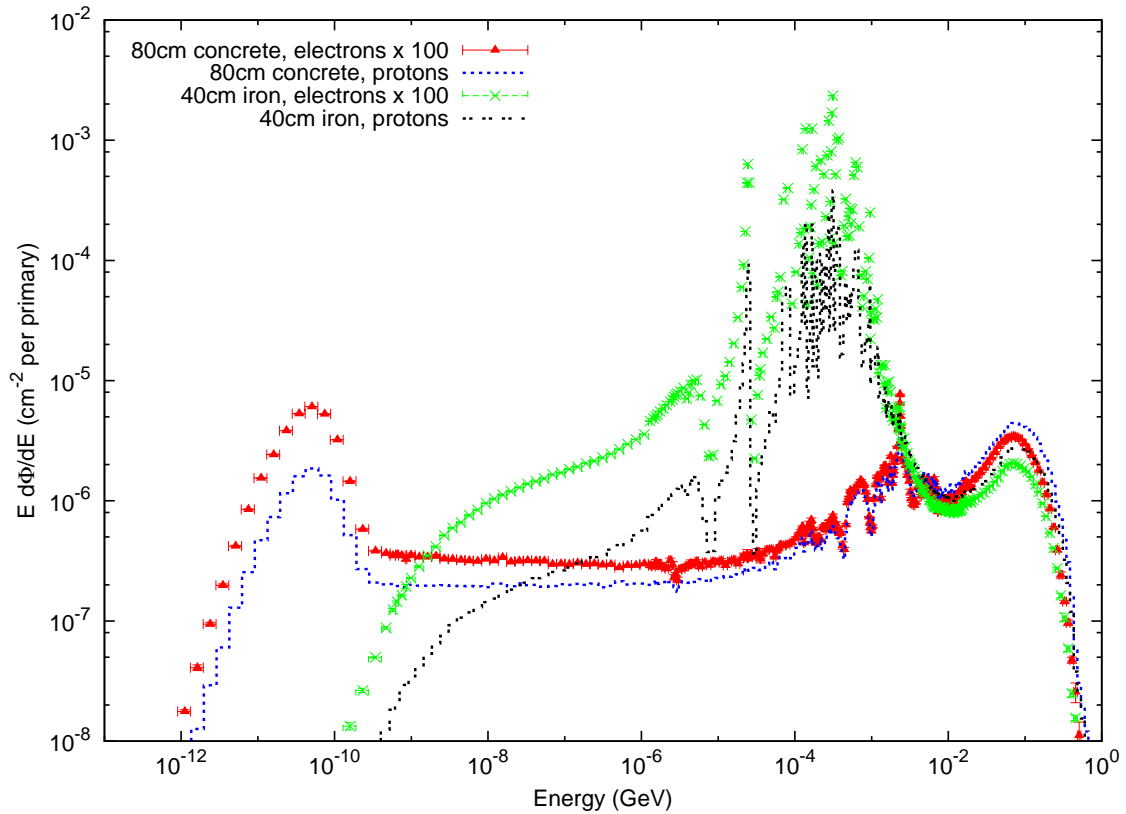


**Figure 30.3:** Neutron energy spectra calculated with the FLUKA code [7,8] from 25 GeV proton and electron beams on a thick copper target. Spectra are evaluated at  $90^\circ$  to the beam direction behind 80 cm of concrete or 40 cm of iron. All spectra are normalized per beam particle. In addition, spectra for electron beam are multiplied by a factor of 100. See full-color version on color pages at end of book.

above 200 MeV. As the cascade through thick shielding is carried by high-energy particles this value is equal to the equilibrium attenuation length at 90 degrees in concrete.

### 30.5. Photon sources

The dose equivalent rate in tissue (in mSv/h) from a gamma point source emitting one photon of energy  $E$  (in MeV) per second at a distance of 1 m is  $4.6 \times 10^{-9} \mu_{en}/\rho E$ , where  $\mu_{en}/\rho$  is the mass energy absorption coefficient. The latter has a value of  $0.029 \pm 0.004 \text{ cm}^2/\text{g}$  for photons in tissue over an energy range between 60 keV and 2 MeV (see Ref. 11 for tabulated values).

Similarly, the dose equivalent rate in tissue (in mSv/h) at the surface of a semi-infinite slab of uniformly activated material containing 1 Bq/g of a gamma emitter of energy  $E$  (in MeV) is  $2.9 \times 10^{-4} R_\mu E$ , where  $R_\mu$  is the ratio of the mass energy absorption coefficients of the photons in tissue and in the material.

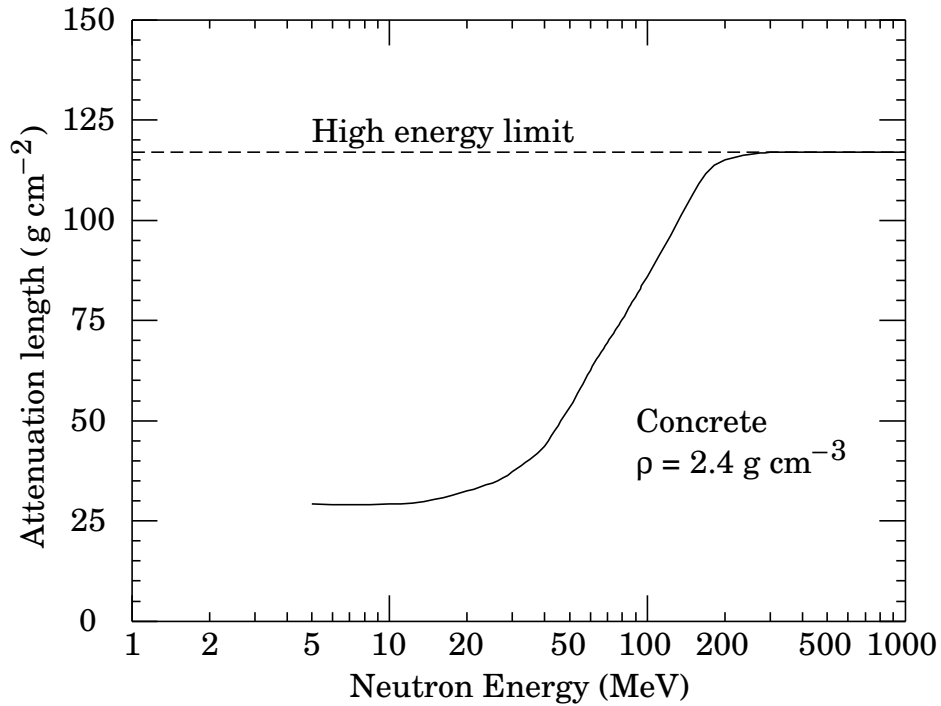


**Figure 30.4:** The variation of the attenuation length for mono-energetic neutrons in concrete as a function of neutron energy [9].

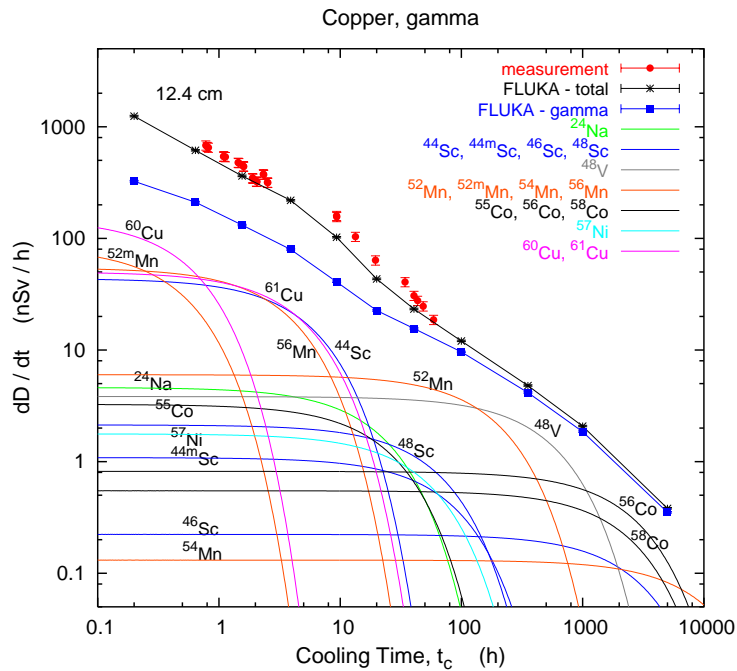


**Figure 30.5:** Contribution of individual gamma-emitting nuclides to the total dose rate at 12.4 cm distance to an activated copper sample [12]. See full-color version on color pages at end of book.



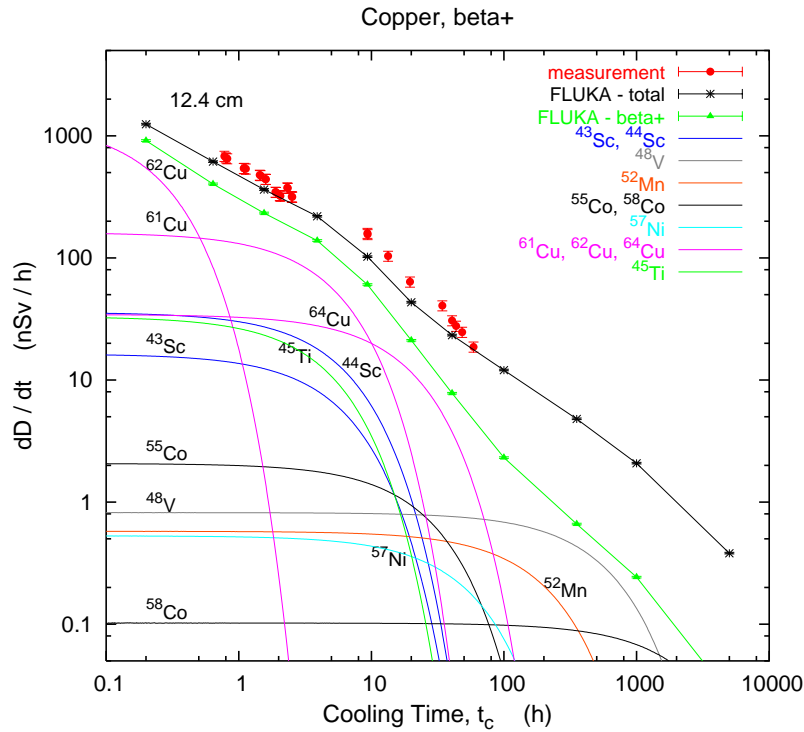


**Figure 30.6:** Contribution of individual positron-emitting nuclides to the total dose rate at 12.4 cm distance to an activated copper sample [12]. See full-color version on color pages at end of book.

### 30.6. Accelerator-induced radioactivity

Typical medium- and long-lived activation products in metallic components of accelerators are  $^{22}\text{Na}$ ,  $^{46}\text{Sc}$ ,  $^{48}\text{V}$ ,  $^{51}\text{Cr}$ ,  $^{54}\text{Mn}$ ,  $^{55}\text{Fe}$ ,  $^{59}\text{Fe}$ ,  $^{56}\text{Co}$ ,  $^{57}\text{Co}$ ,  $^{58}\text{Co}$ ,  $^{60}\text{Co}$ ,  $^{63}\text{Ni}$  and  $^{65}\text{Zn}$ . Gamma-emitting nuclides dominate doses by external irradiation at longer decay times (more than one day) while at short decay times  $\beta^+$  emitters are also important (through photons produced by  $\beta^+$  annihilation). Due to their short range,  $\beta^-$  emitters are relevant, for example, only for dose to the skin and eyes or for doses due to inhalation or ingestion. Fig. 30.5 and Fig. 30.6 show the contributions of gamma and  $\beta^+$  emitters to the total dose rate at 12.4 cm distance to an activated copper sample [12]. Typically, dose rates at a certain decay time are mainly determined by radionuclides having a half-life of the order of the decay time. Extended irradiation periods might be an exception to this general rule as in this case the activity of long-lived nuclides can build up sufficiently so that it dominates that one of short-lived even at short cooling times.

Activation in concrete is dominated by  $^{24}\text{Na}$  (short decay times) and  $^{22}\text{Na}$  (long decay times). Both nuclides can be produced either by low-energy neutron reactions on the sodium-component in the concrete or by spallation reactions on silicon and calcium. At long decay times nuclides of radiological interest in activated concrete can also be  $^{60}\text{Co}$ ,  $^{152}\text{Eu}$ ,  $^{154}\text{Eu}$  and  $^{134}\text{Cs}$ , all of which produced by  $(n,\gamma)$ -reactions with traces of natural cobalt, europium and cesium. Thus, such trace elements might be important even if their

## 10 30. Radioactivity and radiation protection

content in concrete is only a few parts per million or less by weight.

The explicit simulation of radionuclide production with general-purpose Monte Carlo codes has become the most commonly applied method to calculate induced radioactivity and its radiological consequences. Nevertheless, other more approximative approaches, such as “ $\omega$ -factors” [9], can still be useful for fast order-of-magnitude estimates. These  $\omega$ -factors give the dose rate per unit star density (inelastic reactions above a certain energy threshold, *e.g.* 50 MeV) on contact to an extended, uniformly activated object after a 30-day irradiation and 1-day decay. For steel or iron,  $\omega \simeq 3 \times 10^{-12}$  (Sv cm<sup>3</sup>/star). This does not include possible contributions from thermal-neutron activation.

### References:

1. International Commission on Radiation Units and Measurements, *Fundamental Quantities and Units for Ionizing Radiation*, ICRU Report 60 (1998).
2. ICRP Publication 103, *The 2007 Recommendations of the International Commission on Radiological Protection*, Annals of the ICRP, Elsevier (2007).
3. M. Pelliccioni, *Radiation Protection Dosimetry* **88**, 279 (2000).
4. E. Pochin, *Nuclear Radiation: Risks and Benefits*, Clarendon Press, Oxford, 1983.
5. United Nations, *Report of the United Nations Scientific Committee on the Effect of Atomic Radiation*, General Assembly, Official Records A/63/46 (2008).
6. W.P. Swanson, *Radiological Safety Aspects of the Operation of Electron Linear Accelerators*, IAEA Technical Reports Series No. 188 (1979).
7. A. Ferrari, *et al.*, FLUKA, A Multi-particle Transport Code (Program Version 2005), CERN-2005-010 (2005).
8. G. Battistoni, *et al.*, The FLUKA code: Description and benchmarking, *Proceedings of the Hadronic Shower Simulation Workshop 2006*, Fermilab 6–8 September 2006, M. Albrow, R. Raja, eds., *AIP Conference Proceeding 896*, 31–49, (2007).
9. R.H. Thomas and G.R. Stevenson, *Radiological Safety Aspects of the Operation of Proton Accelerators*, IAEA Technical Report Series No. 283 (1988).
10. T.A. Gabriel, *et al.*, *Nucl. Instrum. Methods* **A338**, 336 (1994).
11. <http://physics.nist.gov/PhysRefData/XrayMassCoef/cover.html>.
12. S. Roesler, *et al.*, “Simulation of Remanent Dose Rates and Benchmark Measurements at the CERN-EU High Energy Reference Field Facility,” in *Proceedings of the Sixth International Meeting on Nuclear Applications of Accelerator Technology*, San Diego, CA, 1-5 June 2003, 655–662 (2003).